Exploring Electronic and Conformational Attributes of an Organic Donor-Bridge-Acceptor Molecular System

N. Echeverri, J. D. Perea, S. Leon

To cite this version:

N. Echeverri, J. D. Perea, S. Leon. Exploring Electronic and Conformational Attributes of an Organic Donor-Bridge-Acceptor Molecular System. Adv. Theory Simul. 2025, 8, 2301212.
https://doi.org/10.1002/adts.202301212

Published version.

Published 30 October 2024

Exploring Electronic and Conformational Attributes of an Organic Donor-Bridge-Acceptor Molecular System

Nikolas Echeverri[a], Jose Dario Perea[b]*and Salvador Leon[c]*

Keywords: ZnP-COPV-C_{60} Organic semiconductor; Computational Techniques; Molecular Electronics; Conformational Dynamics; Optoelectronic Materials

Abstract:
This research explores the electronic properties and conformational dynamics of the ZnP-COPV-C_{60} organic semiconductor via specialized Density Functional Theory (DFT) and Molecular Dynamics (MD) computational techniques. First, through DFT calculations, we meticulously dissect essential HOMO, LUMO, and Molecular Electrostatic Potential (MEP) electronic attributes providing insights into the intricate charge transfer processes between the constituent donor-acceptor moieties. Furthermore, MD simulations were employed to unveil the molecular system's multifaceted conformational flexibility and stability. Our Root-mean-squared deviation (RMSD), end-to-end distance, and torsional angles quantitative analysis of conformational attributes support the carbon-bridged oligo-phenylenevinylene (COPV) molecular wire's π-skeleton planar and rigid conformation. This minimal end-to-end distance variation (within ± 1 Å) compared to the initially extended structure and the constrained torsional motion (within $\pm$ 20° for ZnP-COPV and $\pm$ 30° for COPV-C_{60}) after thermalization showcases COPV's ability to maintain structural rigidity over time, aligning with the concept of effective π-conjugation. Finally, through the lens of TD-DFT, we explored the dynamic evolution of the HOMO-LUMO energy gap, TD-DFT excitation energies and oscillator strengths, as the molecular structure transforms over time. Our observed energy gap variation underscores the molecule's adaptability in the face of structural modifications, hinting at an intriguing connection between structural stability and enhanced electronic properties. Our research provides a comprehensive understanding of the intricate interplay between conformational dynamics and electronic attributes in organic semiconductors, providing quantitative insights crucial for designing stable, high-performance materials for cutting-edge optoelectronic applications and helping advance our collective understanding of sustainable energy conversion.

---

[a] Departamento de Física, Universidad del Valle, Cali, 760001, Colombia
[b] Departamento de Bioquímica, Universidad Icesi, Cali, 760001, Colombia
[c] Departamento de Ingeniería Química, Universidad Politécnica de Madrid, Madrid, 28006, Spain
***Email: jdperea@icesi.edu.co, salvador.leon@upm.es**

1. Introduction

Human progress is fundamentally supported by research into functional materials, highlighting the critical role of computational models in creating materials with specific functions in a wide range of biological systems, photovoltaics, and molecular electronics[1]. This synergy between physics, chemistry, materials science, and computer science enhances the exploration of functions and applications in new devices. In addition to intrinsic properties, it is widely acknowledged that exerting control over material structures is indispensable for eliciting their intended functions. While investigating these functions, it becomes apparent that nanoscale structures play a significant role in shaping material properties [2, 3, 4, 5, 6, 7]. The manipulation of material structures is crucial for showcasing material functions, particularly in the realm of Conformational Dynamics and Electronic Properties. These processes underlie the essential mechanisms governing long-distance electronic characteristics in diverse biological and molecular electronics systems. For instance, the electron transfer in π-conjugated molecular wires—a vital facet of these processes—encounters challenges such as limited electron transfer rates (kET) induced by twisting motions along the wire structure. As the wire extends and flexes, there is a transition from coherent tunneling to incoherent hopping, driven by the exponential decay of electronic coupling.

Overcoming these obstacles requires a molecular wire with a rigid, planar structure, which optimizes electronic coupling over long distances. In this context, we focus on carbon-bridged COPVs, a molecular design that features methylene bonds that force the π-orbitals to align in a planar fashion. This strategic alignment, explored in our ZnP-COPV-C_{60} research, is predicted to maximize electronic coupling, positioning COPVs as promising molecular wires for enhanced optoelectronic applications[8, 2, 9]. The unique electronic properties of π-conjugated carbon-based systems such as fullerenes, characterized by their spherical symmetry, have garnered significant attention[10]. These systems exhibit remarkable attributes, including rapid photo-induced charge separation and deliberate deceleration of charge recombination processes[11]. Also, it has been shown that the implementation of Zinc porphyrin (ZnP)[12] as electron donor and its connection to the fullerene by means of a planar π-conjugated molecular bridge with strong electronic coupling may represent a significant increase in photo-induced electron transfer (ET) for organic semiconductor molecular systems[8].

This investigation aims to increase the understanding of the intricate interplay between enhanced electron transfer rates observed in donor-bridge-acceptor organic semiconductors, exemplified by the ZnP-COPV-C_{60} triad (Figure 1), and the structural stability and flexibility of the π-conjugated molecular bridges that link them. Employing cutting-edge computational methodologies like Density Functional Theory (DFT), Time-Dependent Density Functional Theory (TD-DFT), and Molecular Dynamics (MD) simulations, we seek to provide quantitative validation for these relationships. Through meticulous examination, this research significantly propels the frontier of sustainable energy conversion technologies. It provides crucial insights that intricately inform the design of highly efficient organic materials tailored for cutting-edge optoelectronic applications[13]. The exploration of theoretical approximations within this study sparks a compelling dialogue on the potential contributions of computer science to the forefront of advanced physical research.

2. Computational Methods

To investigate the ground-state electronic properties of the ZnP-COPV-C_{60} organic semiconductor, the study was initiated by optimizing the atomic configuration of the molecular system. Density Functional Theory with the Becke-Vosko-Perdew 1986 (BVP86)[14, 15, 16, 17, 18] functional and the 6-31G(d)[19, 20, 21, 22, 23, 24] basis set was employed for a geometry optimization. Considering the molecule's substantial size and the presence of a metal atom, this density functional and basis set were selected as they strike the optimal balance between accuracy and computational cost. This step allowed us to attain the most stable molecular structure, providing key insights into

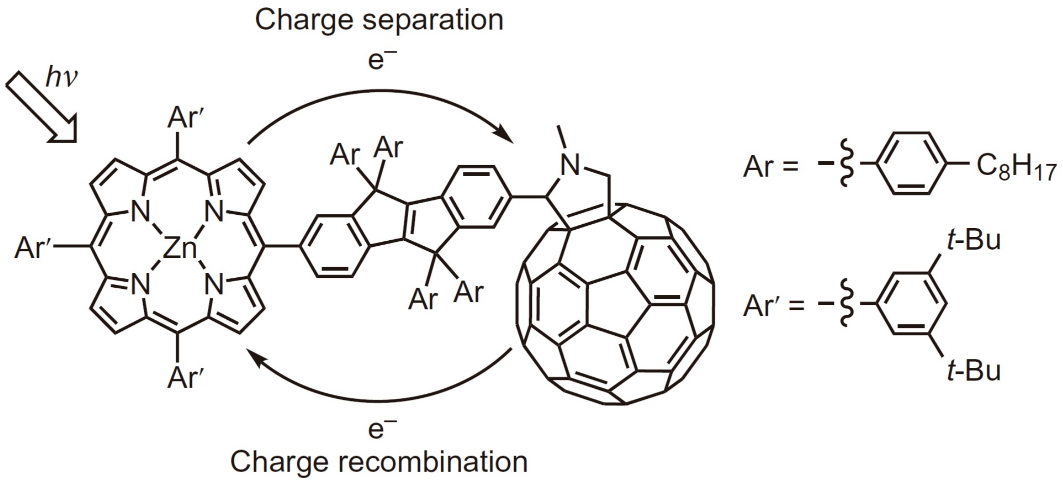

Figure 1. ZnP-COPV-C_{60} molecular system. Reproduced with permission from J. Sukegawa, C. Schubert, X. Zhu, H. Tsuji, D. M. Guldi, and E. Nakamura, (2014) Electron transfer through rigid organic molecular wires enhanced by electronic and electron–vibration coupling, Nature Chemistry. Copyright 2014, Nature Chemistry[8]

the electronic structure. The calculations and visualizations of essential properties, including the Highest Occupied Molecular Orbital (HOMO), Lowest Unoccupied Molecular Orbital (LUMO), and Molecular Electrostatic Potential (MEP), were carried out using Gaussian 09[25] and GaussView 5[26] computer software programs.

To delve deeper into the system's conformational behavior, a classical MD simulation was conducted. This simulation was executed using the LAMMPS[27] program package, utilizing the OPLS[28] force field. The force field parameters describing spatial distances between atoms were initially defined by extracting cartesian coordinates (xyz file) from the DFT-optimized molecular configuration. OPLS force field parameters were generated with the help of PolyParGen[29], a molecular modeling program that simplifies the parameter setup process that precedes MD simulations, by automating the association of atom-specific parameters from preexisting databases. PolyParGen relies on LigParGen[30] and BOSS[31] software packages for this parameter association, and takes in as an input a Chemical Markup Language (cml) file in order to define the respective parameters for the OPLS force field. An important note to make is that, PolyParGen has limitations with complex molecular structures. It can have complications in the process of dividing macromolecules into constituent partial structures when the molecule under examination has cross-linked or large ring structures[29]. Because of this, the program could not generate an OPLS LAMMPS topology file for the entire molecular configuration of the ZnP-COPV-C_{60} system. To overcome this limitation, atomic coordinates from the DFT-optimized structures were manually manipulated, and the system was partitioned into two separate moieties to be used as PolyParGen input files: ZnP and COPV-C_{60}. Additionally, since PolyParGen does not consider metallic atoms like Zinc, the OPLS force field parameters of bond and angular distances associated with this specific element were directly taken from the LAMMPS distribution manual, and manually integrated into the output files to generate the complete molecular topology.

Lennard-Jones and Coulomb non-bonded interactions were calculated within a cutoff radius distance of 10 Å, with a correction for long-range electrostatics using the Ewald summation method (Particle-Particle Particle-Mesh approximation)[32]. To guarantee a stable and equally distributed energy configuration for the dynamics simulation, the system was first relaxed by 10.000 steps of energy minimization. Subsequent production run was executed for a total runtime of 0.1 ns with a timestep of 1.0 fs. The simulation of the dynamics was performed under the NVT ensemble at a constant temperature of 300 K, maintained by the Nose-Hoover thermostat[33, 34] with a damping time of 500 fs. Structural properties of ZnP-COPV-C_{60} were calculated from MD trajectory using VMD molecular visualization software tool[35].

For the analysis of energy level variations concerning the system's dynamic behavior, single point TD-DFT calculations were performed on five distinct geometries extracted from the atomic coordinates observed during the MD trajectory. These calculations were firstly executed using two different range-separated and long-range corrected density functionals that accurately model charge transfer states and excitations, CAM-B3LYP and LC-wPBE, and the same 6-31G(d) basis set as the ground-state geometry optimization. Both functionals have been used on chemically similar structures that have experimental data support (see for instance [36]). To perform a comparative benchmark and properly validate our DFT methodology, additional TD-DFT calculations were executed using the same basis set, and the B3LYP and M06 density functionals[37]. This approach facilitated the determination of variations in the HOMO-LUMO energy gap, TD-DFT excitation energies, and oscillator strengths, as a function of molecular dynamics. The proposed DFT methodology finds direct experimental support from literature (see, for example, figure S1 in the supplementary information of Nakamura et al.[8]), as the observed absorption spectrum for the photo-excitation process of ZnP-COPV-C_{60} exhibits excitation energies similar in numerical value (2.85 eV or 435 nm) to the results obtained for the excitation energies using the CAM-B3LYP functional. Thus, confirming this density functional provides the best agreement with experimental results. A flowchart of our research methodology can be seen in figure 2 below:

3. Results and Discussions

3.1. Ground-State Electronic Properties

Computation of HOMO and LUMO frontier orbitals through the use of Ab-initio electronic structure approach plays a crucial role in molecular-level understanding of ground-state electronic properties of organic semiconductor systems. Identification of relative positions of these orbitals within the molecular structure provides useful insights into the changes in orbital occupancy and thus, information on charge carrier mobility and transport through the material. Previous research has demonstrated the distinct electronic advantages of the constituent components within the well-defined ZnP-COPV-C_{60} donor-bridge-acceptor molecular system, particularly in forming durable charge transfer (CT) states. [2, 12, 38, 39, 40, 41]. Accordingly, the incorporation of chemical modifications in the COPV core might be used to exert influence on electron-vibrational couplings in order to achieve additional nonlinear effects. Additional, ZnP's distinctive behavior as an artificial antenna, which mimics the singlet excitation-energy transfer process inherent in natural photosynthetic reaction centers, and C_{60}'s small reorganization energy, associated with directional control and efficiency in ET reactions, allow for the existence of fast photo-induced charge separation (CS) and slow charge recombination (CR)[42, 43].

From Figure 3, spatial distribution of HOMO and LUMO orbitals on the molecular surface account for the donor/acceptor electronic characteristics previously discussed about ZnP and C_{60} moieties; localization of the HOMO on the ZnP unit and its extension over the π-conjugated molecular wire provides clear evidence on the role of this portion of the molecule as an energy-harvesting moiety, as well as the improved ET because of COPV's strong conjugation and spatial closeness of HOMO and LUMO states. Also, the evident localization of the LUMO on the C_{60} unit showcases fullerene's operation as an electron acceptor.

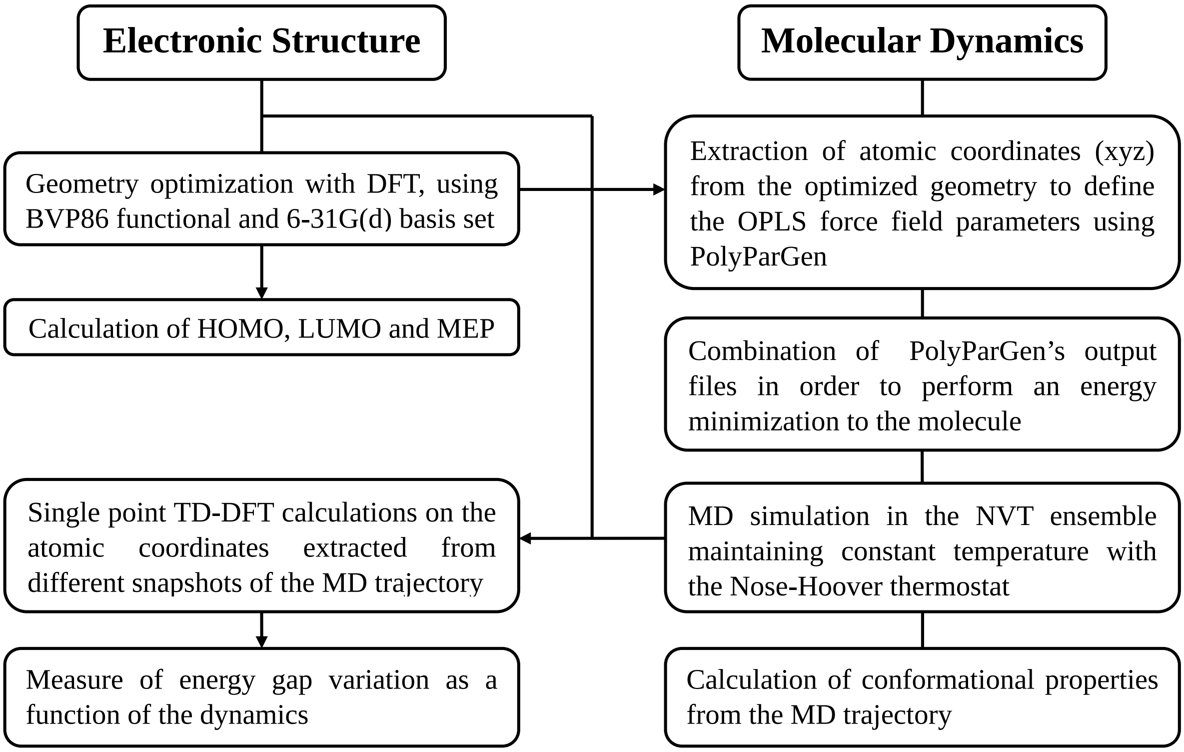

Figure 2. Flowchart of our computational methodology

The computed Molecular Electrostatic Potential (MEP) surface further supports the previous interpretation as it provides insights into the electron density distribution within the molecule[44]. In the case of ZnP-COPV-C_{60} triad, the MEP reveals electron-rich regions, particularly on the C_{60} fullerene, and electron-deficient regions, notably in the Zinc Porphyrin. This dichotomy reinforces the notion of the ZnP radical cation as an electron-donating moiety and the C_{60} radical anion as an electron-accepting component.

3.2. Structural Properties: Conformational Flexibility and Stability

The research conducted by Nakamura and co-workers[8] provides a thorough understanding of the intricate relationship between enhanced ET rate and COPV's rigid/flat structure characteristics. Their study exhibits how strong electronic coupling and inelastic electron tunneling, which are both CS- and CR-enhancing properties, can be explained through COPV'S effective π-conjugation. By employing MD simulations, we provide additional quantitative support for the bridge's π-conjugated nature through the implementation of structural measurements of conformational flexibility and stability of COPV's π-skeleton. MD simulations carried out in our study provide a dynamic understanding of the structural conformation of the organic semiconductor. The calculated MD trajectory provides time-dependent descriptions of the atomic conformation of the molecule, thus encompassing spatial changes in the molecular

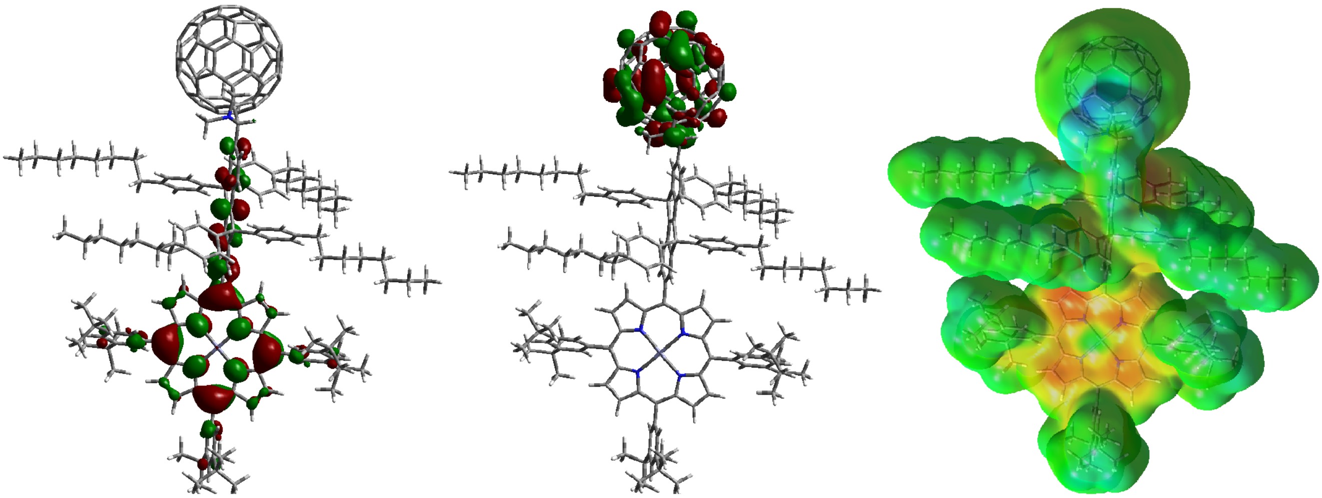

Figure 3. HOMO, LUMO, and MEP Ground-State Electronic Properties of ZnP-COPV-C_{60} Organic Semiconductor: 6-31G(d)/BVP86 level of theory

structure for every timestep of the simulated time interval. From this trajectory, a measurement of ZnP-COPV-C_{60}'s structural stability was obtained by studying the Root-Mean-Squared Deviation (RMSD) of atomic positions in the molecular system (Figure 4). This deviation is employed as a measurement of evolutionary similarity between average atomic distances in the molecule's geometrical arrangement over time. It is used to compare ZnP-COPV-C_{60}'s variation of molecular conformation under dynamic evolution, with the initial geometrical conformation of the energy-minimized structure. Prominent fluctuation of average atomic positions observed in the initial frames of the simulated trajectory can be attributed to the thermal fluctuations inherent in the Nose-Hoover thermostat algorithm used to control temperature in the NVT ensemble. These fluctuations showcase initial adjustment of the system to the simulation conditions. However, despite this initial fluctuating behavior, what is appealing about this measurement is the subsequent stabilization observed when the molecule thermalizes; once it passes frame 25 (25 ps into the simulation), it reaches a state of low variation of the RMSD.

This minimal fluctuation state serves as an initial indicator of the relative rigidity presented by ZnP-COPV-C_{60}. Our analysis of the computed RMSD reveal that atomic positions within the molecular structure experience limited spatial displacement after the molecule stabilizes at a certain temperature. This low conformational change suggests how COPV's π-conjugated structure may contribute to the overall stability of the molecular system under consideration. In order to characterize the molecular wire's connection to the state of low conformational change, we conduct two additional assessments of its flexibility and stability. These evaluations involve measuring the variation in the end-to-end distance and the rotational angles between COPV and its adjacent moieties. These measurements also underscore the molecule's initial thermalization behavior upon thermal fluctuations of the dynamics.

To assess COPV's structural flexibility, we examined the dynamic variation of its end-to-end distance from the computed MD trajectory (Figure 5). This distance represents the spatial separation between the ZnP and C_{60} donor-acceptor moieties over time. Our analysis of this segment distance reveals that, following an initial thermalization period, the system consistently maintains a state of minimal end-to-end distance variation. The small variation in bridge distance, within the narrow range of ± 1 Å compared to the initially extended energy-minimized structure, aligns with Nakamura's statement of COPV's rigidity. This limited spatial distance variation between the donor-acceptor moieties

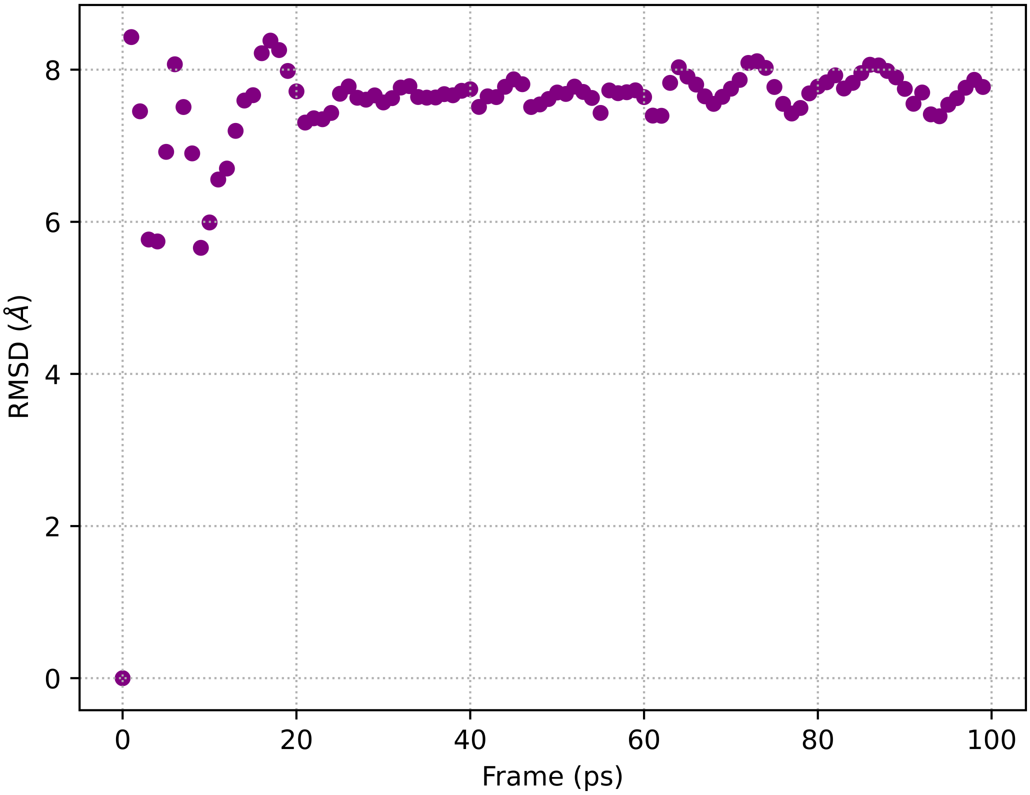

Figure 4. Evaluation of ZnP-COPV-C_{60} structural stability through Root-Mean-Squared Deviation (RMSD) analysis.

demonstrates the rigid structural conformation of the COPV wire, indicating effective π-conjugation that can maintain over time, and further showcasing the conservation of strong electronic coupling.

In order to study rotational stability of the molecular wire, we measured the torsional (dihedral) angle variation around single covalent bonds that connect COPV to ZnP and C_{60} moieties (Figure 6). According to Brédas and co-workers[45], the presence of structural disorder in organic semiconductors, manifested in variable torsion angles between adjacent moieties, influences charge transport dynamics and diminishes the evolution of charge carrier mobility. From these dihedral angle variation measurements, we recognize COPV's constrained torsional motion upon stabilization of the molecule after the initial frames of the simulation. The small variation of torsional motion (between the range of ± 20° for ZnP-COPV and ± 30° for COPV-C_{60}) demonstrates COPV's planar conformation resulting from its π-conjugated nature.

These results are significant, as they provide quantitative justification for COPV's effective π-conjugated nature through the assessment of its rigid and flat structure characteristics. The employed MD simulations confirm this concept by demonstrating how the molecule stabilizes after initial fluctuations and reaches a state of low variation of its structural parameters, thereby reinforcing the idea that COPV's conformational properties play a crucial role in promoting efficient charge transfer in this molecular system.

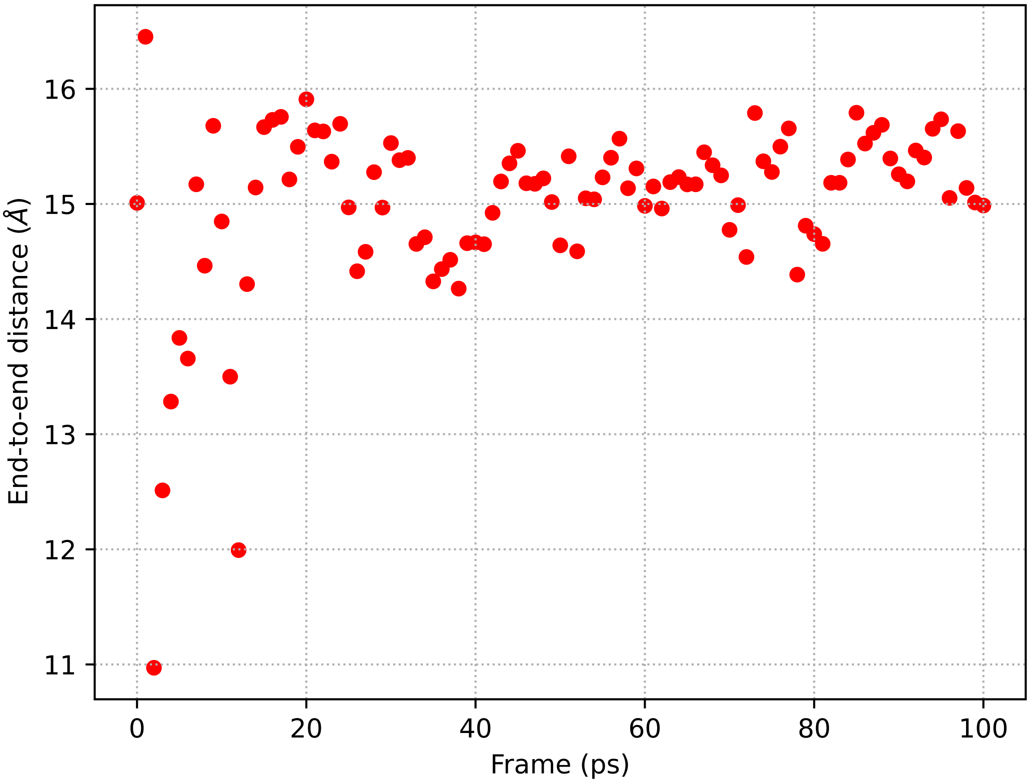

Figure 5. Evaluation of COPV's structural flexibility through end-to-end distance variation.

3.3. *Structural Dynamic Effects on Electronic Properties*

To investigate the interplay between structural dynamics and electronic properties, we performed single-point TD-DFT calculations on five different geometries (snapshots) extracted from the MD trajectory. These five specific snapshots extracted out of the 100 frames of the simulated time interval allowed us to reproduce the effects of geometric distortion throughout the dynamics. As the snapshots were directly taken from the MD trajectory, inheriting the force field parameters of a classical potential, we initially applied a constrained minimization with a limited number of geometry optimization steps. This aimed to ease the degrees of freedom related to bond and angular distances, ensuring parameters align more closely with those typical in a quantum chemistry calculation.

First, the variation of the Molecular Electrostatic Potential (MEP) for the different snapshots was computed (Figure 7). Moreover, atomic charges have been calculated with the CHELPG fitting scheme as implemented in the Multiwfn software[46, 47]. The results of this population analysis reveal that atomic charges do not have strong variations during the MD trajectory. Nevertheless, the charges of the Zinc atom and the Porphyrin Nitrogen atoms across the different snapshots are somewhat larger in absolute value with respect to the initial frame of the MD trajectory (for instance, around 0.9 for the Zinc atom in the later snapshots as compared to 0.67 in the initial frame).

The variation of HOMO-LUMO energy gap across different geometries (Figure 8) provides a compelling observation, as it suggests that the electronic properties of the molecule are not static but change dynamically as the molecular structure evolves during the MD simulation. However, the observed energy gap variation resulting from the molecular

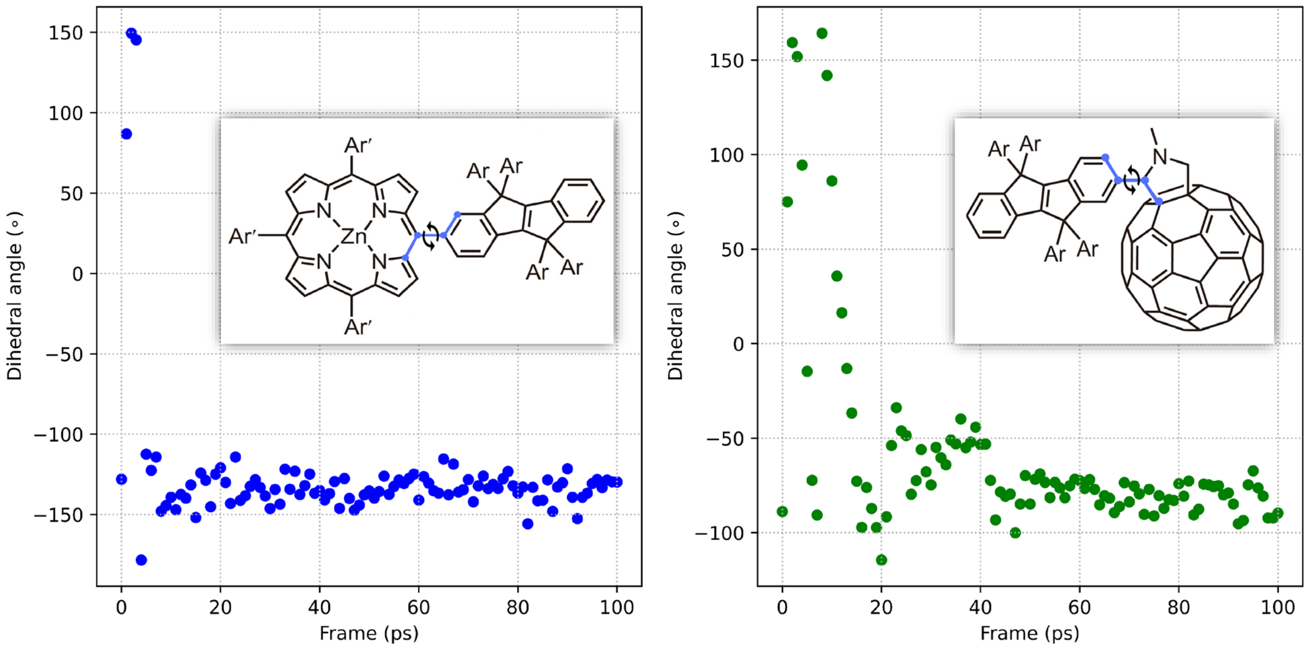

Figure 6. Evaluation of COPV's rotational stability through Dihedral torsion angle variation of single covalent bonds that connect COPV to ZnP (left) and C_{60} (right) moieties.

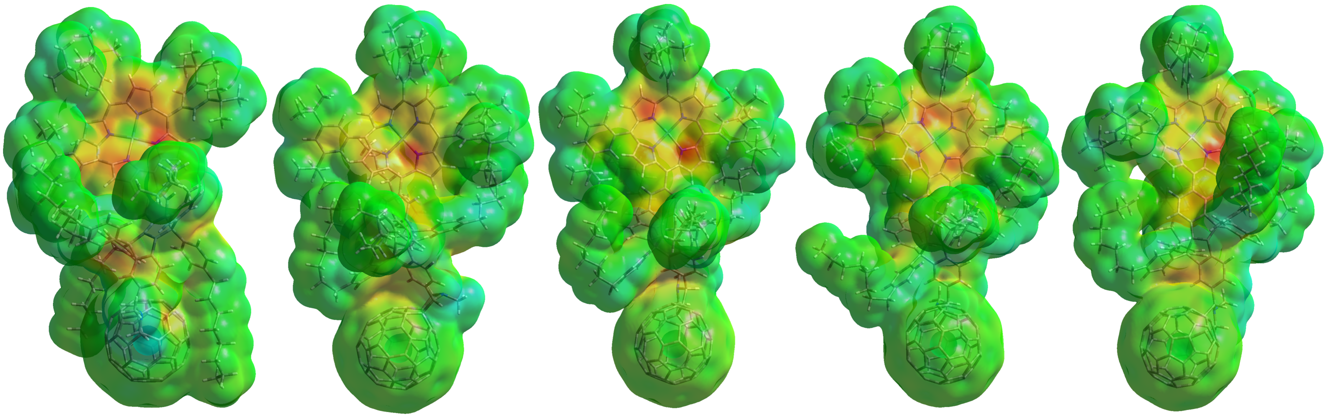

Frame 0 **Frame 25** **Frame 50** **Frame 75** **Frame 95**

Figure 7. MEP for the different snapshots extracted from MD trajectory.

geometries extracted from the simulation showcases no significant dynamic fluctuations. Geometry distortions across the simulated time interval do not cause significant fluctuations in the energy gap, as this value oscillates within a 4-5% range relative to the one for the initial snapshot. Although differences in numerical value of the energy gap are observed for the different functionals, the variation of this value during the simulation along a given trajectory remains within a similar range (except for M06). This dynamic variation in the energy gap is a noteworthy finding, as it reflects the molecule's ability to adapt its electronic properties in response to structural changes, and has several applications similar to previous work done by our group[48, 49].

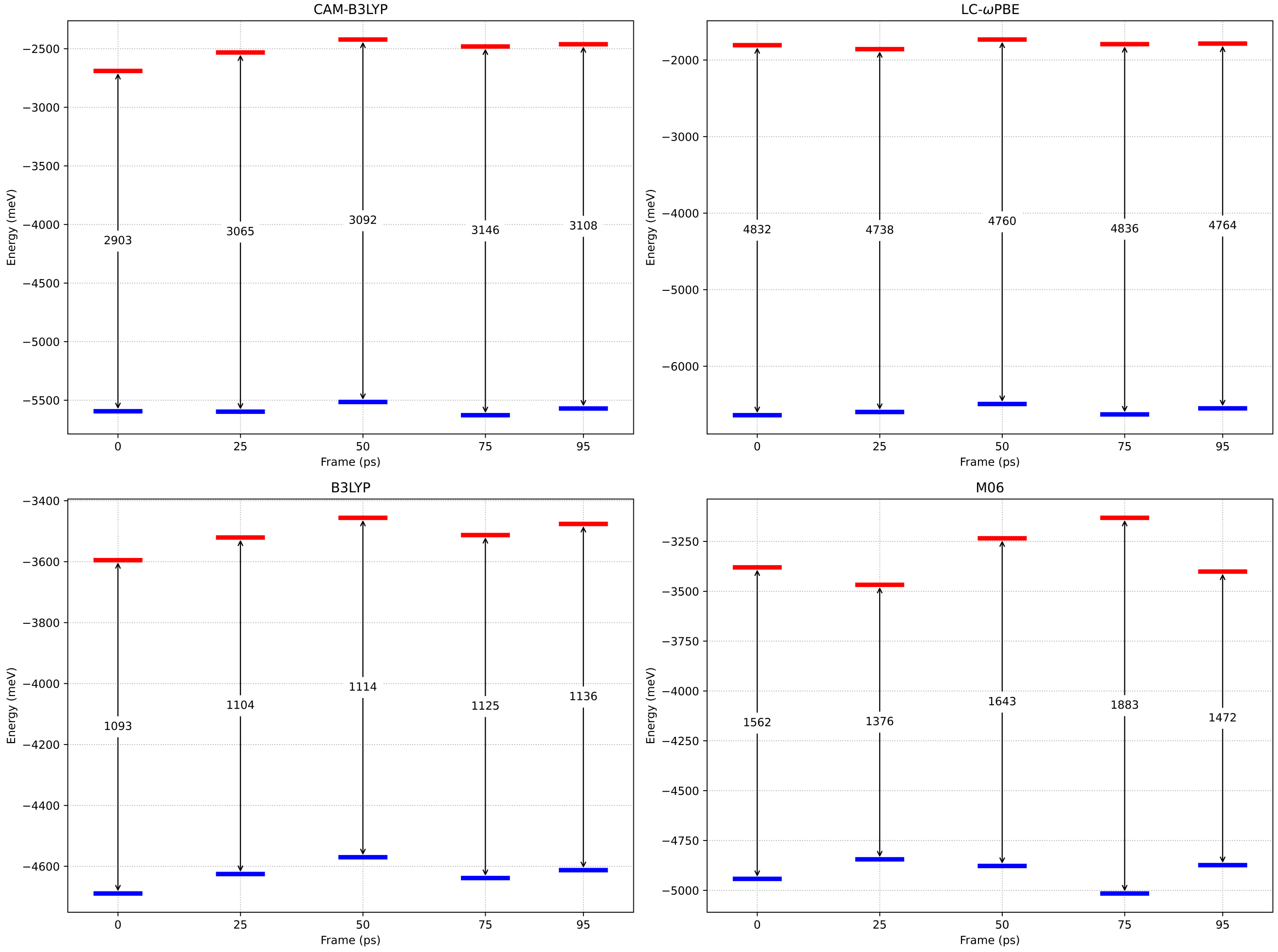

Figure 8. HOMO-LUMO energy gap variation for the different snapshots extracted from MD trajectory.

To gain a deeper insight into the effects of dynamical fluctuations observed during the MD simulation on excitation phenomena and charge transfer, and following previous works such as those by Sumpter and co-workers[50] that have demonstrated the usefulness of this computational approach on similar systems, we carried out TD-DFT calculations to evaluate the variation in excitation energies and oscillator strengths as a function of molecular dynamics (Table 1).

	Frame 0	**Frame 25**	**Frame 50**	**Frame 75**	**Frame 95**
Excitation energy (eV)	1.4327	1.6588	1.6998	1.6330	1.6295
Oscillator strength	0.0137	0.0086	0.0146	0.0131	0.0134

Table 1. TD-DFT excitation energies and oscillator strengths for the different frames extracted from MD trajectory using the CAM-B3LYP density functional.

These results help us understand the spectral properties of the molecule in terms of dynamical change and suggest that it will consistently absorb light at the same wavelengths with predictable intensity, regardless of minor structural fluctuations. The small variation in both parameters observed during the MD simulation suggests that the molecule's optical properties, such as absorption and emission spectra, will be predictable and not highly sensitive to small structural changes or thermal motions.

This reduced variation of the HOMO-LUMO energy gap, as well as in TD-DFT excitation energies and oscillator strengths, implies that as the system equilibrates and the molecule adopts a stable configuration, it transitions to a more consistent electronic state. The stability achieved throughout the dynamics may indicate the system's transition to a more stable charge-separated state, further supporting the concept of efficient charge transfer. This observation suggests a potential link between structural stability and enhanced electronic properties in this molecular system.

The relationship found between structural dynamics and electronic properties has implications for the design and optimization of organic semiconductor materials. By demonstrating how conformational changes impact electronic properties, our research underscores the importance of considering both structural and electronic factors when designing organic semiconductors for optoelectronic applications.

4. Conclusions

In this study, we explored the ground-state electronic properties and structural dynamics of the ZnP-COPV-C_{60} organic semiconductor. Our findings provide insight into the close relationship that exists between structural stability and enhanced electronic performance. We observed the precise spatial distribution of HOMO and LUMO orbitals within the molecular structure. These findings emphasize the unique electronic characteristics of the constituent moieties, with the HOMO localized predominantly on the ZnP unit and the LUMO centered on the C_{60} moiety. This spatial arrangement not only underscores ZnP's role as an energy-harvesting moiety but also highlights the efficient charge transfer capabilities facilitated by the strong conjugation and spatial proximity of HOMO and LUMO states due to COPV. Furthermore, through the application of MD simulations, we observed that the ZnP-COPV-C_{60} system stabilizes after initial fluctuations in structural parameters, demonstrating limited variations in atomic positions. This conformational stability indicates the effectiveness of COPV's π-conjugated structure in maintaining the molecule's structural rigidity over time. The subsequent analysis of the end-to-end distance further corroborated the wire's structural rigidity, showcasing minimal spatial variations between donor and acceptor moieties. Moreover, the measurement of torsional dihedral angles revealed a planar conformation for COPV, emphasizing its π-conjugated nature.

These results underscore the significance of structural stability in enhancing electronic properties. The reduced variation observed in the HOMO-LUMO energy gap, as well as in TD-DFT excitation energies and oscillator strengths, suggests the molecule's transition to a more stable charge-separated state, supporting the concept of efficient charge transfer. This finding holds promise for the design of high-performance organic semiconductors, where optimizing structural parameters can lead to improved charge transport and mobility.

In conclusion, this study offers a foundation for advancing molecular electronics, it encourages researchers to focus on tailored molecular structures that balance stability with electronic efficiency. The insights gained here open doors to the development of next-generation organic semiconductor materials for optoelectronic applications and the integration of molecular electronics into emerging technologies in various industries.

5. Acknowledgments

Authors extend their gratitude to Universidad Del Valle, Universidad Icesi, and Universidad Politécnica de Madrid. Additionally, the authors thank Prof. Dr. Javier Madroñero from the QuanTIC research group for providing valuable computational resources, and to Prof. Dr. Julio Cesar Arce for engaging in fruitful discussions.

6. Author Declaration

The authors have no conflicts to disclose.

References

[1] Lalengmawia Celestine, Renthlei Zosiamliana, Shivraj Gurung, Shalika Ram Bhandari, Amel Laref, Sherzod Abdullaev, and Dibya Prakash Rai. A halide-based perovskite csgex3 (x = cl, br, and i) for optoelectronic and piezoelectric applications. *Advanced Theory and Simulations*, n/a(n/a):2300566, 2023. doi: https://doi.org/10.1002/adts.202300566. URL `https://onlinelibrary.wiley.com/doi/abs/10.1002/adts.202300566`.

[2] Katsuhiko Ariga. Materials nanoarchitectonics for advanced physics research. *Advanced Physics Research*, 2 (7):2200113, 2023. doi: https://doi.org/10.1002/apxr.202200113. URL `https://onlinelibrary.wiley.com/doi/abs/10.1002/apxr.202200113`.

[3] Xiushang Xu, Amogh Kinikar, Marco Di Giovannantonio, Pascal Ruffieux, Klaus Müllen, Roman Fasel, and Akimitsu Narita. On-surface synthesis of dibenzohexacenohexacene and dibenzopentaphenoheptaphene. *Bulletin of the Chemical Society of Japan*, 94(3):997–999, 2021. doi: 10.1246/bcsj.20200382. URL `https://doi.org/10.1246/bcsj.20200382`.

[4] Yoshiaki Sugimoto, Pablo Pou, Masayuki Abe, Pavel Jelinek, Rubén Pérez, Seizo Morita, and Oscar Custance. Chemical identification of individual surface atoms by atomic force microscopy. *Nature*, 446:64–7, 04 2007. doi: 10.1038/nature05530.

[5] Koji Harano. Self-assembly mechanism in nucleation processes of molecular crystalline materials. *Bulletin of the Chemical Society of Japan*, 94(2):463–472, 2021. doi: 10.1246/bcsj.20200333. URL `https://doi.org/10.1246/bcsj.20200333`.

[6] Kensuke Kimura, Kuniyuki Miwa, Hiroshi Imada, Miyabi Imai-Imada, Shota Kawahara, Jun Takeya, Maki Kawai, Michael Galperin, and Yousoo Kim. Selective triplet exciton formation in a single molecule. *Nature*, 570, 06 2019. doi: 10.1038/s41586-019-1284-2.

[7] Eiichi Nakamura. Atomic-resolution transmission electron microscopic movies for study of organic molecules, assemblies, and reactions: The first 10 years of development. *Accounts of Chemical Research*, 50(6):1281–1292, 2017. doi: 10.1021/acs.accounts.7b00076. URL `https://doi.org/10.1021/acs.accounts.7b00076`. PMID: 28481074.

[8] Junpei Sukegawa, Christina Schubert, Xiaozhang Zhu, Hayato Tsuji, Dirk M. Guldi, and Eiichi Nakamura. Electron transfer through rigid organic molecular wires enhanced by electronic and electron–vibration coupling. *Nature Chemistry*, 6(10):899–905, 2014. doi: 10.1038/nchem.2026.

[9] Hayato Tsuji. Carbon-bridged oligo(phenylenevinylene)s that reveal cryogenic phenomena at room temperature. *Bulletin of the Chemical Society of Japan*, 95(4):657–662, 2022. doi: 10.1246/bcsj.20220041. URL `https://doi.org/10.1246/bcsj.20220041`.

[10] Nazario Martín, Luis Sánchez, Beatriz Illescas, and Ignacio Pérez. C60-based electroactive organofullerenes. *Chemical Reviews*, 98(7):2527–2548, 1998. doi: 10.1021/cr9701039. URL `https://doi.org/10.1021/cr9701039`. PMID: 11848970.

[11] Hiroshi Imahori and Yoshiteru Sakata. Donor-linked fullerenes: Photoinduced electron transfer and its potential application. *Advanced Materials*, 9:537–546, 1997.

[12] Mandeep K. Chahal, Habtom B. Gobeze, Whitney A. Webre, Paul A. Karr, Daniel T. Payne, Katsuhiko Ariga, Francis D'Souza, and Jonathan P. Hill. Electron and energy transfer in a porphyrin–oxoporphyrinogen–fullerene triad, znp–oxp–c60. *Phys. Chem. Chem. Phys.*, 22:14356–14363, 2020. doi: 10.1039/D0CP02696D. URL `http://dx.doi.org/10.1039/D0CP02696D`.

[13] Alexandre Vercouter, Vincent Lemaur, Claudio Melis, and Jérôme Cornil. Computing the lattice thermal conductivity of small-molecule organic semiconductors: A systematic comparison of molecular dynamics based methods. *Advanced Theory and Simulations*, 6(5):2200892, 2023. doi: https://doi.org/10.1002/adts.202200892. URL `https://onlinelibrary.wiley.com/doi/abs/10.1002/adts.202200892`.

[14] P. Hohenberg and W. Kohn. Inhomogeneous electron gas. *Phys. Rev.*, 136:B864–B871, 11 1964. doi: 10.1103/PhysRev.136.B864. URL `https://link.aps.org/doi/10.1103/PhysRev.136.B864`.

[15] W. Kohn and L. J. Sham. Self-consistent equations including exchange and correlation effects. *Phys. Rev.*, 140:A1133–A1138, 11 1965. doi: 10.1103/PhysRev.140.A1133. URL `https://link.aps.org/doi/10.1103/PhysRev.140.A1133`.

[16] S. H. Vosko, L. Wilk, and M. Nusair. Accurate spin-dependent electron liquid correlation energies for local spin density calculations: a critical analysis. *Canadian Journal of Physics*, 58(8):1200–1211, 1980. doi: 10.1139/p80-159. URL `https://doi.org/10.1139/p80-159`.

[17] A. D. Becke. A multicenter numerical integration scheme for polyatomic molecules. *The Journal of Chemical Physics*, 88(4):2547–2553, 02 1988. ISSN 0021-9606. doi: 10.1063/1.454033. URL `https://doi.org/10.1063/1.454033`.

[18] John P. Perdew. Density-functional approximation for the correlation energy of the inhomogeneous electron gas. *Phys. Rev. B*, 33:8822–8824, 01 1986. doi: 10.1103/PhysRevB.33.8822. URL `https://link.aps.org/doi/10.1103/PhysRevB.33.8822`.

[19] R. Ditchfield, W. J. Hehre, and J. A. Pople. Self-Consistent Molecular-Orbital Methods. IX. An Extended Gaussian-Type Basis for Molecular-Orbital Studies of Organic Molecules. *The Journal of Chemical Physics*, 54 (2):724–728, 01 1971. doi: 10.1063/1.1674902.

[20] W. J. Hehre, R. Ditchfield, and J. A. Pople. Self—Consistent Molecular Orbital Methods. XII. Further Extensions of Gaussian—Type Basis Sets for Use in Molecular Orbital Studies of Organic Molecules. *The Journal of Chemical Physics*, 56(5):2257–2261, 09 2003. ISSN 0021-9606. doi: 10.1063/1.1677527. URL `https://doi.org/10.1063/1.1677527`.

[21] P.C. Hariharan and J.A. Pople. Accuracy of ah n equilibrium geometries by single determinant molecular orbital theory. *Molecular Physics*, 27(1):209–214, 1974. doi: 10.1080/00268977400100171. URL `https://doi.org/10.1080/00268977400100171`.

[22] Günther W. Spitznagel, Timothy Clark, Paul von Ragué Schleyer, and Warren J. Hehre. An evaluation of the performance of diffuse function-augmented basis sets for second row elements, na-cl. *Journal of Computational Chemistry*, 8(8):1109–1116, 1987. doi: https://doi.org/10.1002/jcc.540080807. URL `https://onlinelibrary.wiley.com/doi/abs/10.1002/jcc.540080807`.

[23] Timothy Clark, Jayaraman Chandrasekhar, Günther W. Spitznagel, and Paul Von Ragué Schleyer. Efficient diffuse function-augmented basis sets for anion calculations. iii. the 3-21+g basis set for first-row elements, li–f. *Journal of Computational Chemistry*, 4(3):294–301, 1983. doi: https://doi.org/10.1002/jcc.540040303. URL `https://onlinelibrary.wiley.com/doi/abs/10.1002/jcc.540040303`.

[24] Michael J. Frisch, John A. Pople, and J. Stephen Binkley. Self-consistent molecular orbital methods 25. Supplementary functions for Gaussian basis sets. *The Journal of Chemical Physics*, 80(7):3265–3269, 04 1984. ISSN 0021-9606. doi: 10.1063/1.447079. URL `https://doi.org/10.1063/1.447079`.

[25] Michael J. Frisch. Gaussian 09, Revision A.1. *Revision A.1*, 2009. Gaussian Inc. Wallingford CT.

[26] M. J. Frisch, G. W. Trucks, H. B. Schlegel, G. E. Scuseria, M. A. Robb, J. R. Cheeseman, G. Scalmani, V. Barone, G. A. Petersson, H. Nakatsuji, X. Li, M. Caricato, A. V. Marenich, J. Bloino, B. G. Janesko, R. Gomperts, B. Mennucci, H. P. Hratchian, J. V. Ortiz, A. F. Izmaylov, J. L. Sonnenberg, D. Williams-Young, F. Ding, F. Lipparini, F. Egidi, J. Goings, B. Peng, A. Petrone, T. Henderson, D. Ranasinghe, V. G. Zakrzewski, J. Gao, N. Rega, G. Zheng, W. Liang, M. Hada, M. Ehara, K. Toyota, R. Fukuda, J. Hasegawa, M. Ishida, T. Nakajima, Y. Honda, O. Kitao, H. Nakai, T. Vreven, K. Throssell, J. A. Montgomery, Jr., J. E. Peralta, F. Ogliaro, M. J. Bearpark, J. J. Heyd, E. N. Brothers, K. N. Kudin, V. N. Staroverov, T. A. Keith, R. Kobayashi, J. Normand, K. Raghavachari, A. P. Rendell, J. C. Burant, S. S. Iyengar, J. Tomasi, M. Cossi, J. M. Millam, M. Klene, C. Adamo, R. Cammi, J. W. Ochterski, R. L. Martin, K. Morokuma, O. Farkas, J. B. Foresman, and D. J. Fox. Gaussian 16 Revision C.01, 2016. Gaussian Inc. Wallingford CT.

[27] Aidan P. Thompson, H. Metin Aktulga, Richard Berger, Dan S. Bolintineanu, W. Michael Brown, Paul S. Crozier, Pieter J. in 't Veld, Axel Kohlmeyer, Stan G. Moore, Trung Dac Nguyen, Ray Shan, Mark J. Stevens, Julien Tranchida, Christian Trott, and Steven J. Plimpton. Lammps - a flexible simulation tool for particle-based materials modeling at the atomic, meso, and continuum scales. *Computer Physics Communications*, 271:108171, 2022. ISSN 0010-4655. doi: https://doi.org/10.1016/j.cpc.2021.108171. URL `https://www.sciencedirect.com/science/article/pii/S0010465521002836`.

[28] Michael J. Robertson, Yue Qian, Matthew C. Robinson, Julian Tirado-Rives, and William L. Jorgensen. Development and testing of the opls-aa/m force field for rna. *Journal of Chemical Theory and Computation*, 15(4):2734–2742, 2019. doi: 10.1021/acs.jctc.9b00054. URL `https://doi.org/10.1021/acs.jctc.9b00054`. PMID: 30807148.

[29] Makoto YABE, Kazuki MORI, Kazuyoshi UEDA, and Minoru TAKEDA. Development of polypargen software to facilitate the determination of molecular dynamics simulation parameters for polymers. *Journal of Computer Chemistry, Japan -International Edition*, 5:2018–0034, 2019. doi: 10.2477/jccjie.2018-0034.

[30] Leela S. Dodda, Israel Cabeza de Vaca, Julian Tirado-Rives, and William L. Jorgensen. LigParGen web server: an automatic OPLS-AA parameter generator for organic ligands. *Nucleic Acids Research*, 45(W1):W331–W336, 04 2017. ISSN 0305-1048. doi: 10.1093/nar/gkx312. URL `https://doi.org/10.1093/nar/gkx312`.

[31] William L. Jorgensen and Julian Tirado–Rives. Molecular modeling of organic and biomolecular systems using boss and mcpro. *Journal of Computational Chemistry*, 26(16):1689–1700, 2005. doi: https://doi.org/10.1002/jcc.20297. URL `https://onlinelibrary.wiley.com/doi/abs/10.1002/jcc.20297`.

[32] Joan J. Cerdà, V. Ballenegger, and C. Holm. Particle-particle particle-mesh method for dipolar interactions: On error estimates and efficiency of schemes with analytical differentiation and mesh interlacing. *The Journal of Chemical Physics*, 135(18):184110, 11 2011. ISSN 0021-9606. doi: 10.1063/1.3657407. URL `https://doi.org/10.1063/1.3657407`.

[33] Shūichi Nosé. A molecular dynamics method for simulations in the canonical ensemble. *Molecular Physics*, 52 (2):255–268, 1984. doi: 10.1080/00268978400101201. URL `https://doi.org/10.1080/00268978400101201`.

[34] William G. Hoover. Canonical dynamics: Equilibrium phase-space distributions. *Phys. Rev. A*, 31:1695–1697, 03 1985. doi: 10.1103/PhysRevA.31.1695. URL `https://link.aps.org/doi/10.1103/PhysRevA.31.1695`.

[35] William Humphrey, Andrew Dalke, and Klaus Schulten. Vmd: Visual molecular dynamics. *Journal of Molecular Graphics*, 14(1):33–38, 1996. ISSN 0263-7855. doi: https://doi.org/10.1016/0263-7855(96)00018-5. URL `https://www.sciencedirect.com/science/article/pii/0263785596000185`.

[36] Li-Na Wu, Ming-Yue Sui, Song Xiao, Yu-Zhong Xie, and Guang-Yan Sun. Design of single-porphyrin donors toward high open-circuit voltage for organic solar cells via an energy level gradient-distribution screening strategy of fragments: a theoretical study. *Phys. Chem. Chem. Phys.*, 22:4015–4022, 2020. doi: 10.1039/C9CP04903G. URL `http://dx.doi.org/10.1039/C9CP04903G`.

[37] Baris Temelli, Ozgun Ozasik, and Dilek Yüksel. Synthesis, spectroscopic properties, and dft calculations of imine-bridged meso–meso- and -meso-linked porphyrin–corrole dyads. *European Journal of Organic Chemistry*, 2017(33):4905–4915, 2017. doi: https://doi.org/10.1002/ejoc.201700896. URL `https://chemistry-europe.onlinelibrary.wiley.com/doi/abs/10.1002/ejoc.201700896`.

[38] Michael R. Wasielewski. Photoinduced electron transfer in supramolecular systems for artificial photosynthesis. *Chemical Reviews*, 92(3):435–461, 1992. doi: 10.1021/cr00011a005. URL `https://doi.org/10.1021/cr00011a005`.

[39] Yuqi Hou, Xue Zhang, Kepeng Chen, Dongyi Liu, Zhijia Wang, Qingyun Liu, Jianzhang Zhao, and Antonio Barbon. Charge separation, charge recombination, long-lived charge transfer state formation and intersystem crossing in organic electron donor/acceptor dyads. *J. Mater. Chem. C*, 7:12048–12074, 2019. doi: 10.1039/C9TC04285G. URL `http://dx.doi.org/10.1039/C9TC04285G`.

[40] Bo Albinsson, Mattias P. Eng, Karin Pettersson, and Mikael U. Winters. Electron and energy transfer in donor–acceptor systems with conjugated molecular bridges. *Phys. Chem. Chem. Phys.*, 9:5847–5864, 2007. doi: 10.1039/B706122F. URL `http://dx.doi.org/10.1039/B706122F`.

[41] Devens Gust, Thomas A. Moore, and Ana L. Moore. *Mimicking Bacterial Photosynthesis*, chapter 10, pages 187–210. John Wiley and Sons, Ltd, 2005. ISBN 9783527606740. doi: https://doi.org/10.1002/3527606742.ch10. URL `https://onlinelibrary.wiley.com/doi/abs/10.1002/3527606742.ch10`.

[42] Dirk M. Guldi. Fullerenes: three dimensional electron acceptor materials. *Chem. Commun.*, pages 321–327, 2000. doi: 10.1039/A907807J. URL `http://dx.doi.org/10.1039/A907807J`.

[43] Yasuyuki Araki and Osamu Ito. Factors controlling lifetimes of photoinduced charge-separated states of fullerene-donor molecular systems. *Journal of Photochemistry and Photobiology C: Photochemistry Reviews*, 9(3): 93–110, 2008. ISSN 1389-5567. doi: https://doi.org/10.1016/j.jphotochemrev.2008.04.004. URL `https://www.sciencedirect.com/science/article/pii/S138955670800052X`.

[44] Cherumuttathu H. Suresh, Geetha S. Remya, and Puthannur K. Anjalikrishna. Molecular electrostatic potential analysis: A powerful tool to interpret and predict chemical reactivity. *WIREs Computational Molecular Science*, 12(5):e1601, 2022. doi: https://doi.org/10.1002/wcms.1601. URL `https://wires.onlinelibrary.wiley.com/doi/abs/10.1002/wcms.1601`.

[45] Veaceslav Coropceanu, Jérôme Cornil, Demetrio A. da Silva Filho, Yoann Olivier, Robert Silbey, and Jean-Luc Brédas. Charge transport in organic semiconductors. *Chemical Reviews*, 107(4):926–952, 2007. doi: 10.1021/cr050140x. URL `https://doi.org/10.1021/cr050140x`. PMID: 17378615.

[46] Tian Lu and Feiwu Chen. Multiwfn: A multifunctional wavefunction analyzer. *Journal of Computational Chemistry*, 33(5):580–592, 2012. doi: https://doi.org/10.1002/jcc.22885. URL `https://onlinelibrary.wiley.com/doi/abs/10.1002/jcc.22885`.

[47] Jun Zhang and Tian Lu. Efficient evaluation of electrostatic potential with computerized optimized code. *Phys. Chem. Chem. Phys.*, 23:20323–20328, 2021. doi: 10.1039/D1CP02805G. URL `http://dx.doi.org/10.1039/D1CP02805G`.

[48] Pascal Friederich, Salvador León, José Darío Perea, Loïc M Roch, and Alán Aspuru-Guzik. The influence of sorbitol doping on aggregation and electronic properties of pedot:pss: a theoretical study. *Machine Learning: Science and Technology*, 2(1):01LT01, dec 2020. doi: 10.1088/2632-2153/ab983b. URL `https://dx.doi.org/10.1088/2632-2153/ab983b`.

[49] Patrick Reiser, Manuel Konrad, Artem Fediai, Salvador Léon, Wolfgang Wenzel, and Pascal Friederich. Analyzing dynamical disorder for charge transport in organic semiconductors via machine learning. *Journal of Chemical Theory and Computation*, 17(6):3750–3759, 2021. doi: 10.1021/acs.jctc.1c00191. URL `https://doi.org/10.1021/acs.jctc.1c00191`. PMID: 33944566.

[50] Lei Wang, Jacek Jakowski, Sophya Garashchuk, and Bobby G. Sumpter. Understanding how isotopes affect charge transfer in p3ht/pcbm: A quantum trajectory-electronic structure study with nonlinear quantum corrections. *Journal of Chemical Theory and Computation*, 12(9):4487–4500, 2016. doi: 10.1021/acs.jctc.6b00126. URL `https://doi.org/10.1021/acs.jctc.6b00126`. PMID: 27504981.